ESD-TR-82-002

(12)

Technical Report

592

W. Rotman
J.C. Lee

Dielectric Lens Antenna for EHF Airborne Satellite Communication Terminals

16 February 1982

Prepared for the Department of the Air Force
under Electronic Systems Division Contract F19628-80-C-0002 by

Lincoln Laboratory
MASSACHUSETTS INSTITUTE OF TECHNOLOGY
LEXINGTON, MASSACHUSETTS

DISCLAIMER NOTICE

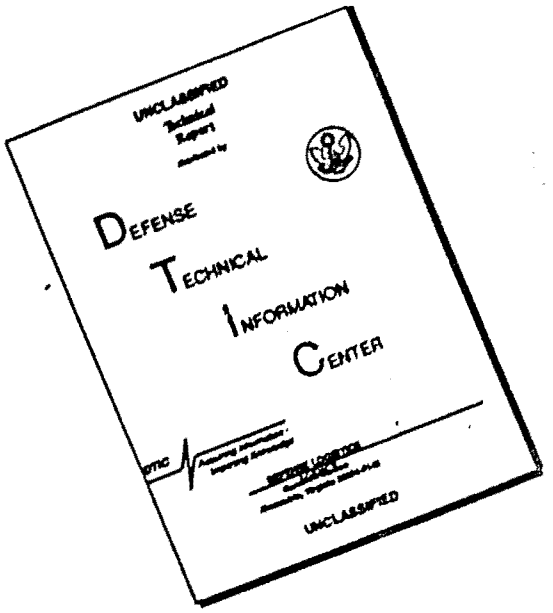

THIS DOCUMENT IS BEST QUALITY AVAILABLE. THE COPY FURNISHED TO DTIC CONTAINED A SIGNIFICANT NUMBER OF PAGES WHICH DO NOT REPRODUCE LEGIBLY.

MASSACHUSETTS INSTITUTE OF TECHNOLOGY
LINCOLN LABORATORY

DIELECTRIC LENS ANTENNA FOR EHF AIRBORNE SATELLITE COMMUNICATION TERMINALS

W. ROTMAN
J.C. LEE
Group 61

TECHNICAL REPORT 592

16 FEBRUARY 1982

LEXINGTON MASSACHUSETTS

ABSTRACT

A mechanically-steerable dielectric lens antenna, suitable for installation in an EHF airborne MILSATCOM terminal on high performance aircraft, was designed and tested. The antenna system consists of a six-inch diameter plano/convex lens with a dual frequency feed (43.5-45.5 GHz for the uplink and 20.2-21.2 GHz for the downlink). The measured gain and half-power beamwidths of the antenna system are 35.5 dB and 3.2° for the uplink (44.5 GHz) and 29.5 dB and 6.0° for the downlink (20.7 GHz), corresponding to overall aperture efficiencies of 71% and 81%, respectively. The first sidelobes are -18 dB for the downlink and -20 dB for the uplink while the corresponding far-out sidelobes are less than -26 dB and -34 dB, respectively, for all angles beyond 18°. These characteristics are compatible with a high ECCM capability for an antenna of this size in an aircraft.

CONTENTS

LIST OF ILLUSTRATIONS

LIST OF TABLES

I. INTRODUCTION

In connection with Lincoln Laboratory programs to develop EHF technology[1] for military satellite communication systems, millimeter-wave antennas were investigated for potential application to airborne satellite communication terminals. Several different lens and reflector configurations are currently under study. The model which is the subject of this report consists of a combination of a scalar horn feed with a dielectric lens collimator. The characteristics required from these antennas include:

1. Essentially complete coverage of the hemisphere above the horizontal plane of the aircraft.

2. Dual-frequency operation as a transmitting antenna in the 43.5 to 45.5 GHz uplink band and as a receiving antenna in the 20.2 to 21.2 GHz downlink band.

3. Effective gain at least equivalent to that of a six inch aperture antenna, assuming 50% aperture efficiency (greater than 27 dB at 20.5 GHz and 34 dB at 44.5 GHz, including radome losses).

4. Operation over the entire 5% bandwidth in each of the two frequency ranges without retuning.

In addition, the antennas are designed for circular polarization, although this is not a requirement.

The choice of antenna configuration to satisfy these requirements is critically dependent upon several conflicting factors. High-performance aircraft (i.e., fighter/bombers, such as the F-111/A) require either flush-mounted or minimally-protrusive antenna systems to reduce aerodynamic drag and turbulence effects. Conformal phased arrays[2] and hybrid-scan arrays (which are mechanically rotated in azimuth and phase-scanned in elevation) have been extensively investigated for this application. However, the gain of any flush-mounted antenna, mounted on top of the aircraft fuselage, decreases from its broadside value by as much as ten decibels in scanning from the zenith to the horizon[3]. In addition, phased-array antennas typically have dissipative

losses of three to four decibels in their feed networks and phase shifters. As a result, flush-mounted arrays are much larger and more complex than mechanically-steered aperture antennas of equivalent performance. Also, hybrid-scan arrays are only partially conformal and require radomes since they are built as flat plate structures which are not aerodynamically integral with the contours of the airframe.

The system designer is likewise faced with the choice between reflectors and lenses for the aperture antenna. At SHF frequencies the reflector is the obvious selection since a dielectric lens would generally be too heavy. However, at millimeter wavelengths the absence of aperture blockage and its adverse effects on the radiation characteristics give an advantage to lens systems, particularly for electrically-small apertures and dual-frequency feeds which tend to be larger than their single frequency counterparts.

The antenna system selected for development (shown conceptually in Fig. 1) consists of a plano/convex polystyrene (Rexolite) lens of six-inch diameter, fed by a dual-frequency corrugated horn feed. The lens is secured to the feed by a shroud which also shields the antenna from unwanted radiation incident from the rear sector. The shroud is partially lined with a thin absorber to attenuate internal reflections from the lens and radome surfaces. (This absorber was not used in the radiation pattern measurements shown in this report, but might have beneficial effects on sidelobes in an aircraft installation.) The corrugated horn, or scalar feed, which was originally developed as the illuminator for a two-foot offset paraboloid reflector in a mobile (SCOTT) terminal* for armored personnel carriers, has almost equal E- and H-plane radiation patterns and provides a satisfactory aperture illumination over the lens for good control of sidelobes on both the uplink and downlink bands.

---

*Details of the feed design, construction and test will be reported by one of the authors (J. C. Lee) in a Lincoln Laboratory Technical Report with the tentative title, "A Dual Frequency Offset Reflector Antenna for SCOTT Applications".

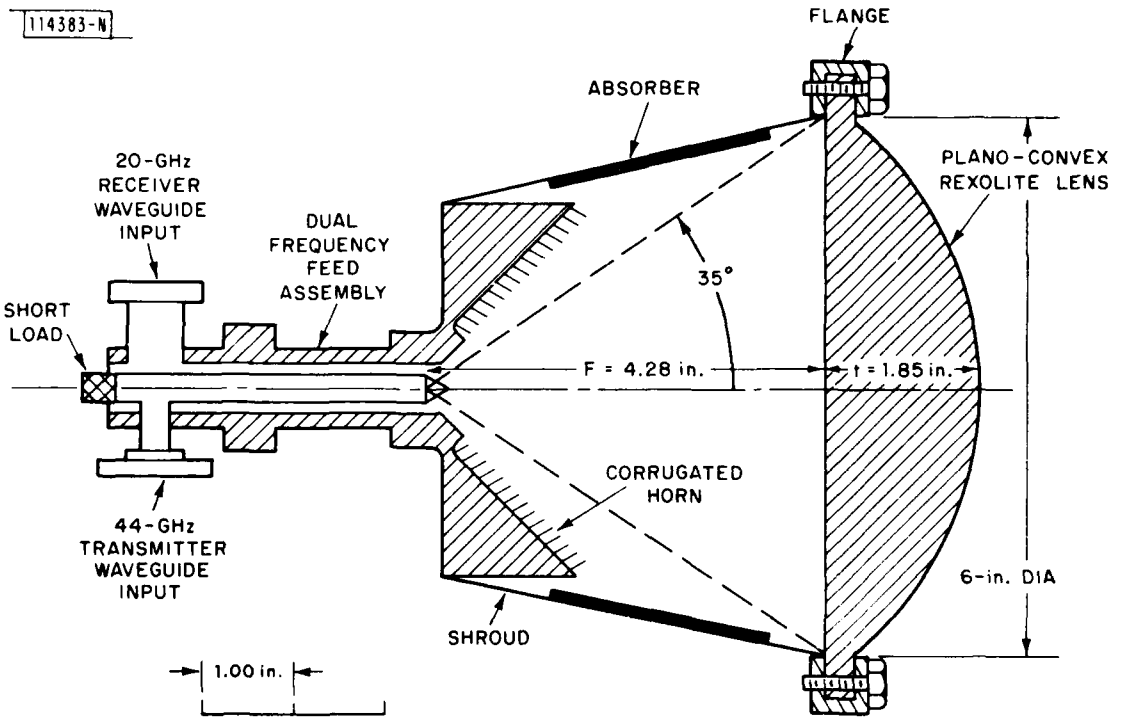

Fig. 1. Dual frequency (20/44 GHz) lens antenna.

The rationale for the choice of a plano-convex lens with the planar side facing the feed is given in Appendix I of Reference 4. Of the two lens shapes which are easy to analyze[5], the plano-convex lens with the convex side toward the feed tends to increase the amplitude taper and decrease sidelobes by bunching the energy from the feed towards the center of the lens, but has relatively large angles of incidence for rays on the curved side and corresponding high reflections for, at least, one sense of linear polarization. The second type of lens, which has a curved inner surface coinciding with the input spherical phase front from the feedhorn, bunches the energy at the edges of the lens, decreasing the amplitude taper and increasing the sidelobes. Both of these lenses have the disadvantage that one surface coincides with a wavefront so that surface reflections are focussed back to the feedhorn, possibly causing an adverse impedance mismatch.

On the other hand, the plano-convex lens with the plane side facing the feed has several desirable characteristics. Since refraction takes place at both surfaces, the angles of incidence are relatively small, leading to small reflections for any incident polarization. Similarly, reflections from the lens into the feed tend to be small since neither lens is equi-phased. Finally, the lens has little effect on the amplitude taper since it is intermediate in geometry between the two cases previously discussed.

II. DUAL-FREQUENCY FEED SYSTEM

The feed consists of a single corrugated (scalar) horn which is optimized for the two frequency bands, with two concentric waveguide openings at the horn throat (Fig. 2). The inner circular waveguide is used for the uplink transmitting (43.5-45.5 GHz) band and the outer coaxial waveguide for the downlink (20.2-21.2 GHz). Separate circular polarizers, orthomode transducers, and impedance-matching elements are designed and integrated compactly into these waveguides. The overall length of the feed is less than 5 inches; its largest cross-section is the horn opening which is about 4 inches in diameter.

The design requirements for the antenna feed are: low cost, compact size, rugged construction and low sidelobes in both frequency bands. Ideally, the feed radiation characteristics should approximate a Huygen's source radiator[6] with equal E-plane and H-plane amplitude and phase patterns in order to control the off-axis polarization characteristics of the lens. Although a Huygen's source can be realized by multi-flare or multi-mode horns, the corrugated horn generally has superior polarization qualities over a broad band[7]. Similarly, other types of diplex feed systems[6] were considered for this application, but were generally found to be either more complex or incapable of operating in two frequency bands which are separated by a ratio of over two to one.

Electrical characteristics of this corrugated horn feed are shown in Figs. 3 through 7. For the transmitting frequencies the return loss at the waveguide input terminals (Fig. 3B) is greater than 15 dB (VSWR<1.45) over the entire 43.5-45.5 GHz band. The match (Fig. 3A) for its orthomode transducer transition between the rectangular and circular waveguide sections is better than 20 dB (VSWR<1.25). A resistive termination in the circular waveguide (Fig. 2), that serves to absorb unwanted reflected energy from the horn and lens (which is of the orthogonal sense of circular polarization from the transmitted wave), has a return loss (Fig. 3C) greater than 17 dB over the band (VSWR<1.35). The axial ratio of the dielectric polarizer in the circular

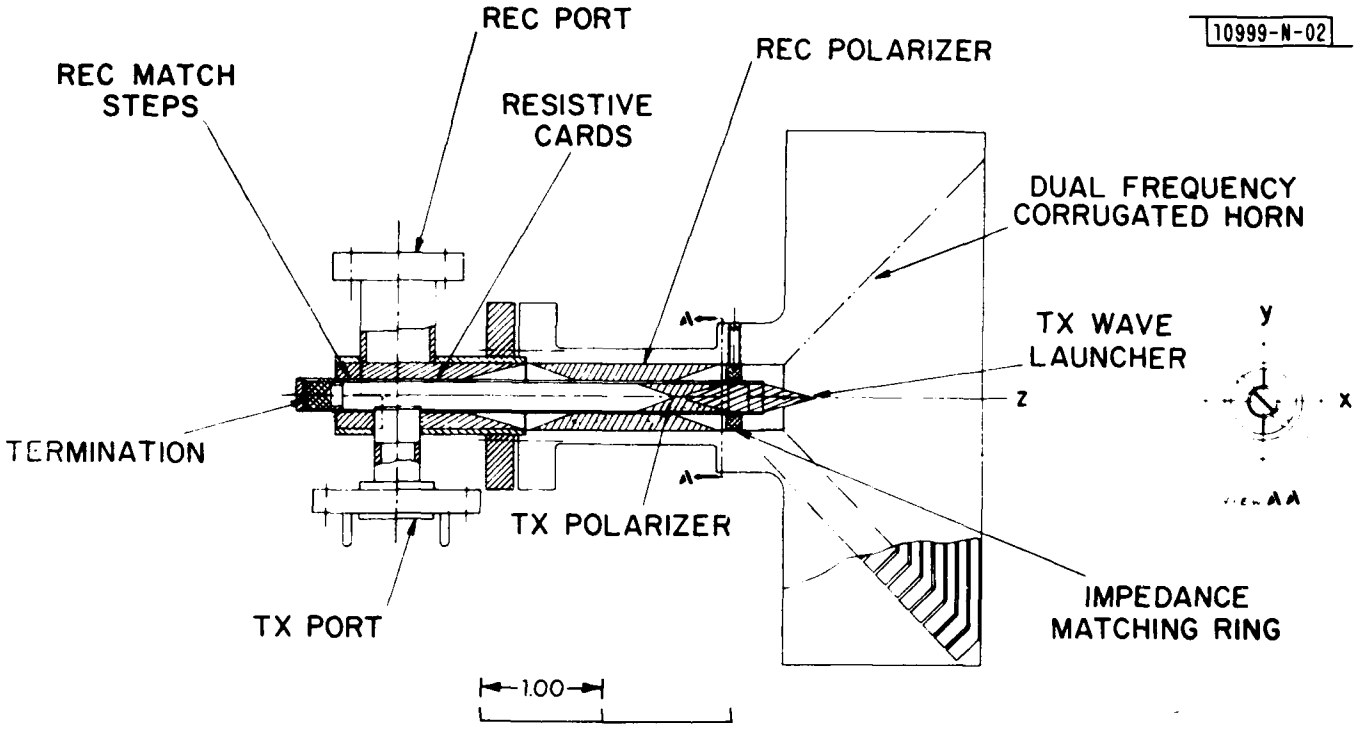

Fig. 2. Dual frequency feed assembly.

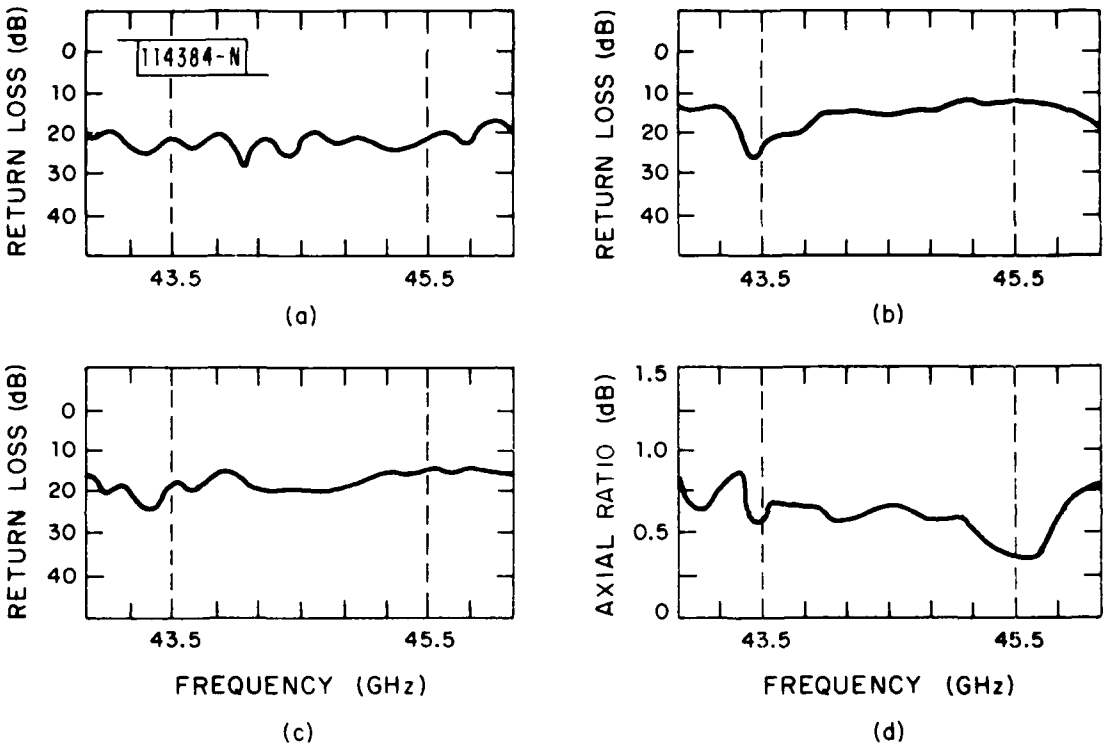

Fig. 3. Dual frequency feed, transmitting components: (a) Match of orthomode transducer, (b) Match at waveguide input, (c) Match of short load, (d) Axial ratio of polarizer.

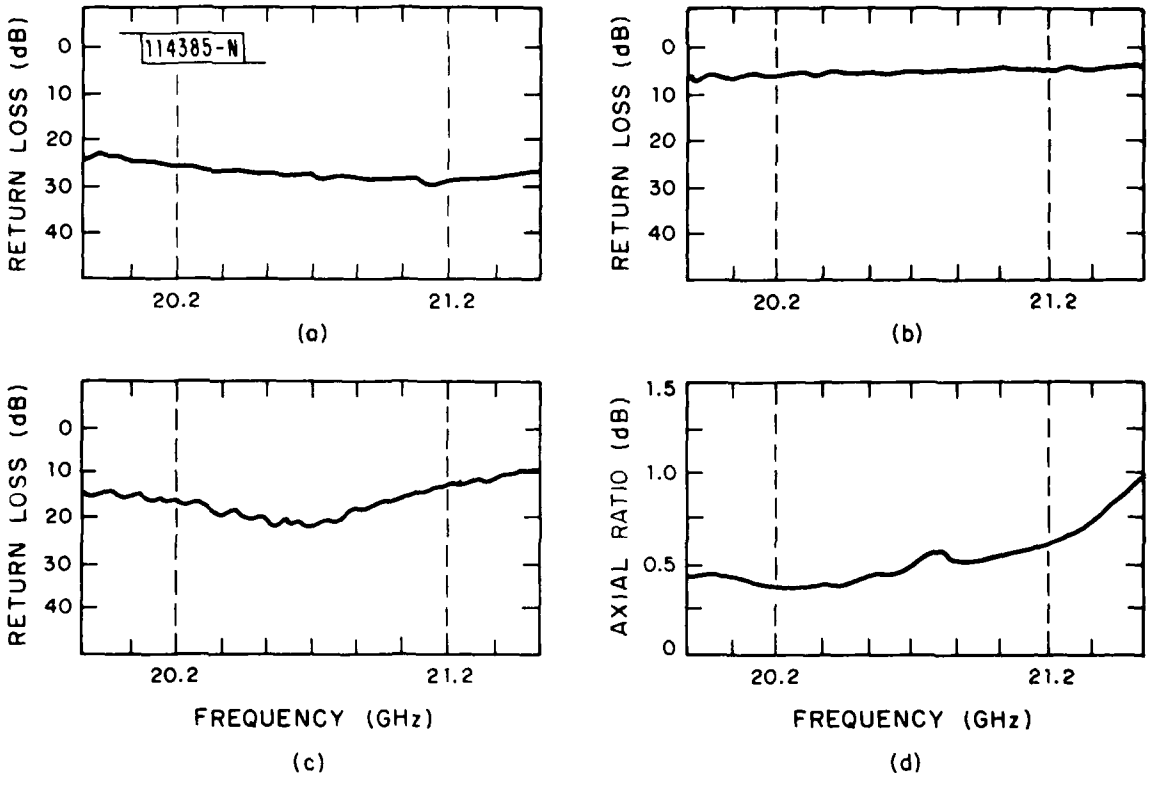

Fig. 4. Dual frequency feed, receiving components: (a) Match of orthomode transducer, (b) Match at waveguide input, (c) Match without tuning ring, (d) Axial ratio of polarizer.

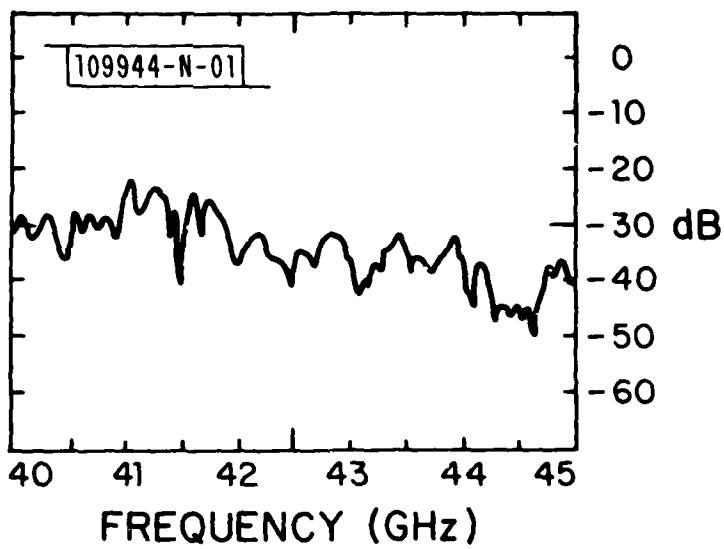

Fig. 5. Isolation between transmitter and receiver terminals of dual-frequency feed.

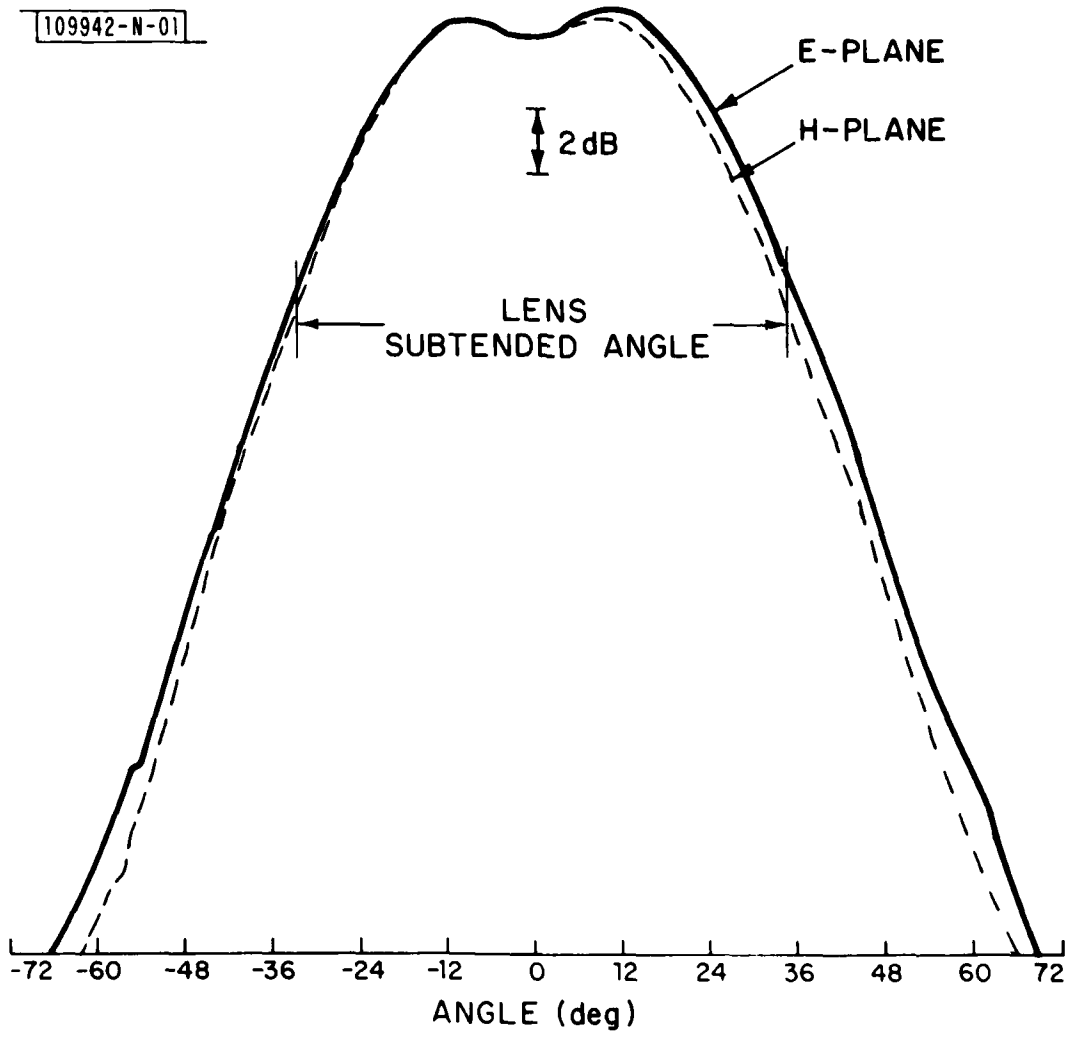

Fig. 6. Feed radiation patterns at receiver center frequency (20.7 GHz).

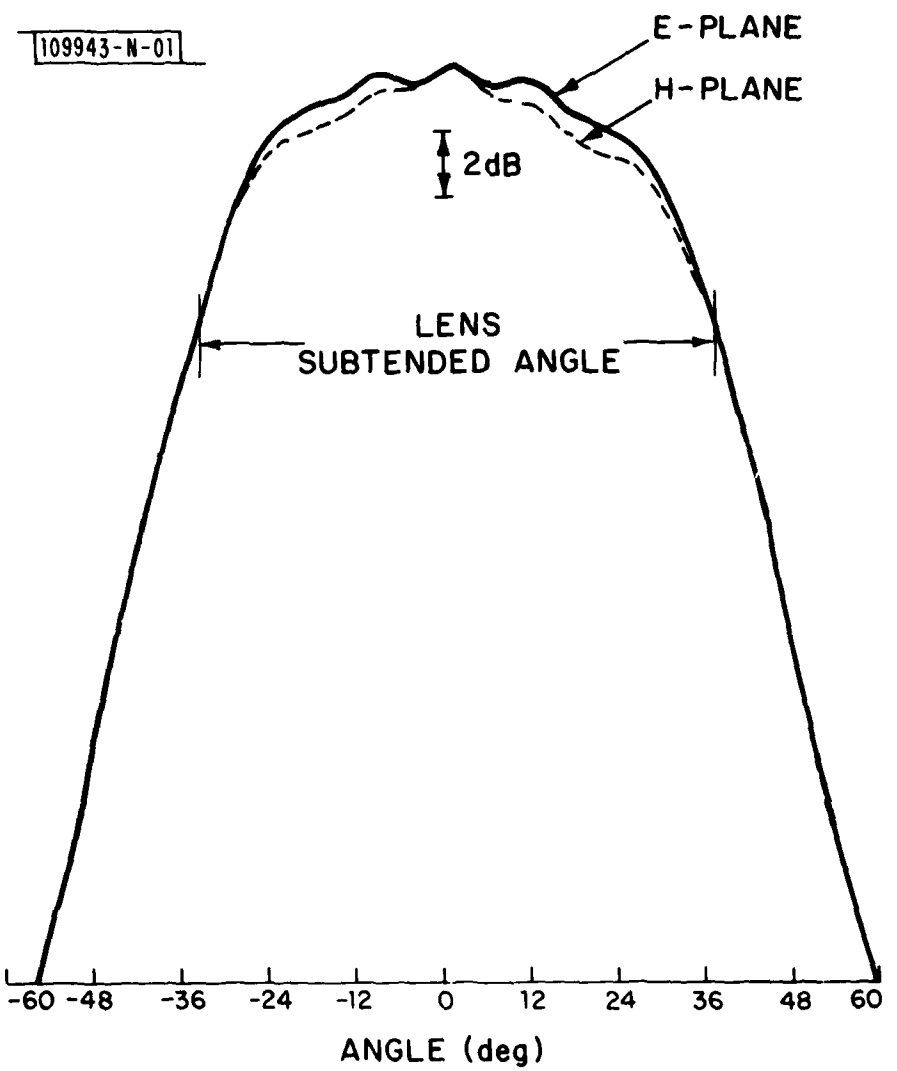

Fig. 7. Feed radiation patterns at transmitter center frequency (44.5 GHz).

waveguide (Tx POLARIZER of Fig. 2), which is a principal factor in determining the polarization of the transmitted wave, is less than one dB over the band (Fig. 3D). This corresponds to a polarization loss of less than 0.1 dB for the uplink.

For the downlink the return loss at the receiver's waveguide output terminal at the feed is greater than 13 dB (VSWR<1.60) over the 20.2 to 21.2 GHz band (Fig. 4B). This result is obtained, with the aid of an impedance-matching ring (Fig. 2), from an initially uncompensated return loss which was as poor as 3 dB (VSWR<6.0; Fig. 4C). The return loss of the orthomode transition from the receiver's input to the coaxial waveguide section of the feed is matched to a return loss of 23 dB (VSWR<1.20; Fig. 3A). The axial ratio of the feed on reception, as determined by the receiver's dielectric polarizer, is likewise less than one dB (Fig. 4D). The mutual coupling between the transmitter output and receiver terminal on the feed is relatively low, being less than -30 dB over the uplink band. Fig. 5 shows the isolation from 40 to 45 GHz. The portion of the uplink band between 45 and 45.5 GHz is not shown, but is likewise below the -30 dB limit. This degree of isolation assures satisfactory decoupling between the uplink and downlink signals.

Although the transmitting and receiving radiation patterns for this feed were originally optimized for the SCOTT reflector application, they are equally well suited for the airborne terminal lens requirements. Within each frequency band the E- and H-plane feed patterns (Figs. 6 and 7) are almost identical, with the illumination down by eight dB at the edge of the lens ($\theta=\pm 35°$) from its on-axis value. The characteristic features of the aperture illumination functions and the corresponding far-field radiation patterns for the lens, computed from these feed illuminations, will be discussed after presentation of the design equations for the lens contours.

III. DESIGN EQUATIONS FOR PLANO/CONVEX LENS

The parametric expressions for the coordinates (x,r) of the lens-generating curve (Fig. 8) are derived from Snell's Law and the equality of path lengths ($P_{01}+P_{12}+P_{23}$=Constant) from the focal point through the lens as[4]:

$$x = \frac{F\cos\psi(\cos\theta-1) + t\cos\theta\cos\psi(\eta-1)}{\cos\theta(\eta-\cos\psi)} \tag{1}$$

$$r = \frac{F\sin\theta(\eta^2-\eta\cos\psi+\cos\theta-1) + t\cos\theta\sin\theta(\eta-1)}{\eta\cos\theta(\eta-\cos\psi)} \tag{2}$$

$$\eta\sin\psi = \sin\theta \tag{3}$$

where (Fig. 8):

θ is the angle of incidence

ψ is the angle of refraction

η is the index of refraction

F is the focal length

t is the lens thickness at center, given by

$$\frac{t}{D} = \frac{[(F/D)+1/4]^{1/2} - F/D}{\eta-1} \tag{4}$$

and D is the lens diameter. Evaluation of Eqn. (4) for η=1.59 (polystyrene) shows that F/D cannot be much less than unity to maintain a reasonably small value of lens thickness.

The ratio of the amplitude distribution $A(\theta)$ of the feed to the amplitude distribution over the lens aperture F(r) is given by[4]

$$\frac{F(r)}{A(\theta)} = (\eta F+t)\left[\frac{\sin\theta\cos\theta(\eta-\cos\psi)}{\eta r U}\right]^{1/2} \tag{5}$$

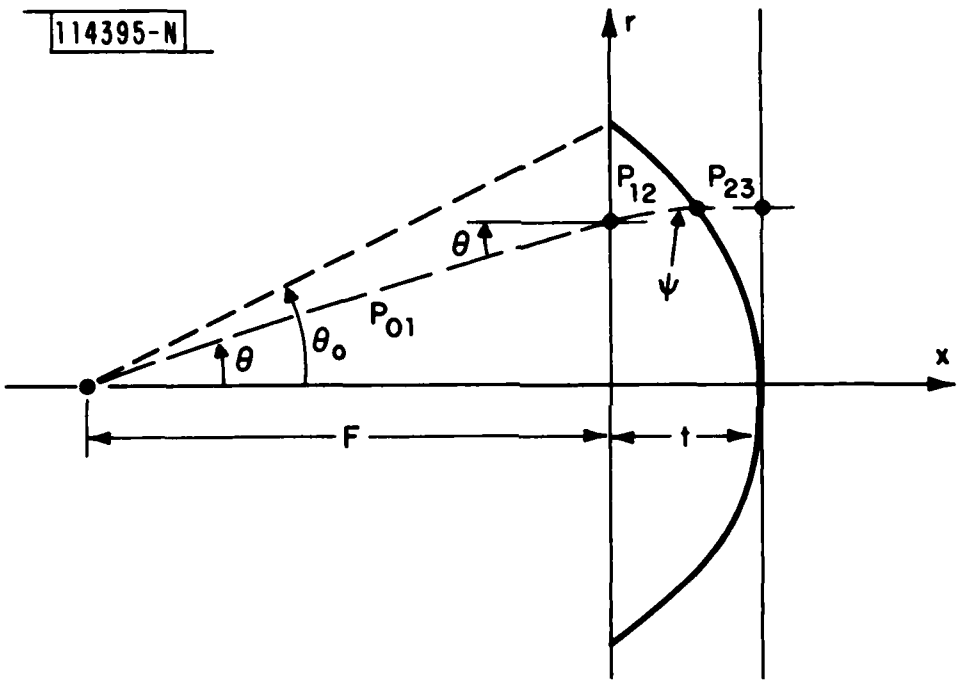

Fig. 8. Geometry of plano-convex lens.

where $U = F\cos\theta(n^2-\cos\psi+\cos\theta-1) - F\sin\theta(\sin\theta-\cos\theta\tan\psi)$

$$+ t(n-1)\cos 2\theta + nr\sin\theta(n-\cos\psi) - r\cos^2\theta\tan\psi$$

For the present design, the distance D (Fig. 8) between the points where the lens thickness goes to zero is larger than the diameter of the lens aperture (6.5" versus 6"D) in order to provide an attachment rim. The focal length F is 4.28" (θ_o=35°, F/D=0.658), which gives a center thickness t of 1.85". The amplitude ratio F(r)/A(θ), calculated from Eqns. (1-5) using these parameters and with n=1.59, is close to unity (Fig. 9) over the entire lens radius (0.9 dB at the rim).

The theoretical radiation patterns for the lens with its scalar feed are calculated from the equation[8]:

$$g(u) = \int_0^1 F(\tilde{r})\, J_o(u\tilde{r})\, \tilde{r}\, d\tilde{r} \qquad (6)$$

where $r = r/r_o$ = normalized lens radius

$u = 2\pi r \sin\theta/\lambda$

$J_o(x)$ = zero order Bessel function.

The aperture distributions F(r) for the lens are obtained from the measured feed patterns A(θ) of Figs. 6 and 7, as modified by the amplitude ratio F(r)/A(θ) of Fig. 9. These values are used to compute the theoretical radiation patterns of the lens (Figs. 10 and 11) for the uplink transmitting (44.5 GHz) and downlink receiving (20.7 GHz) center frequencies.

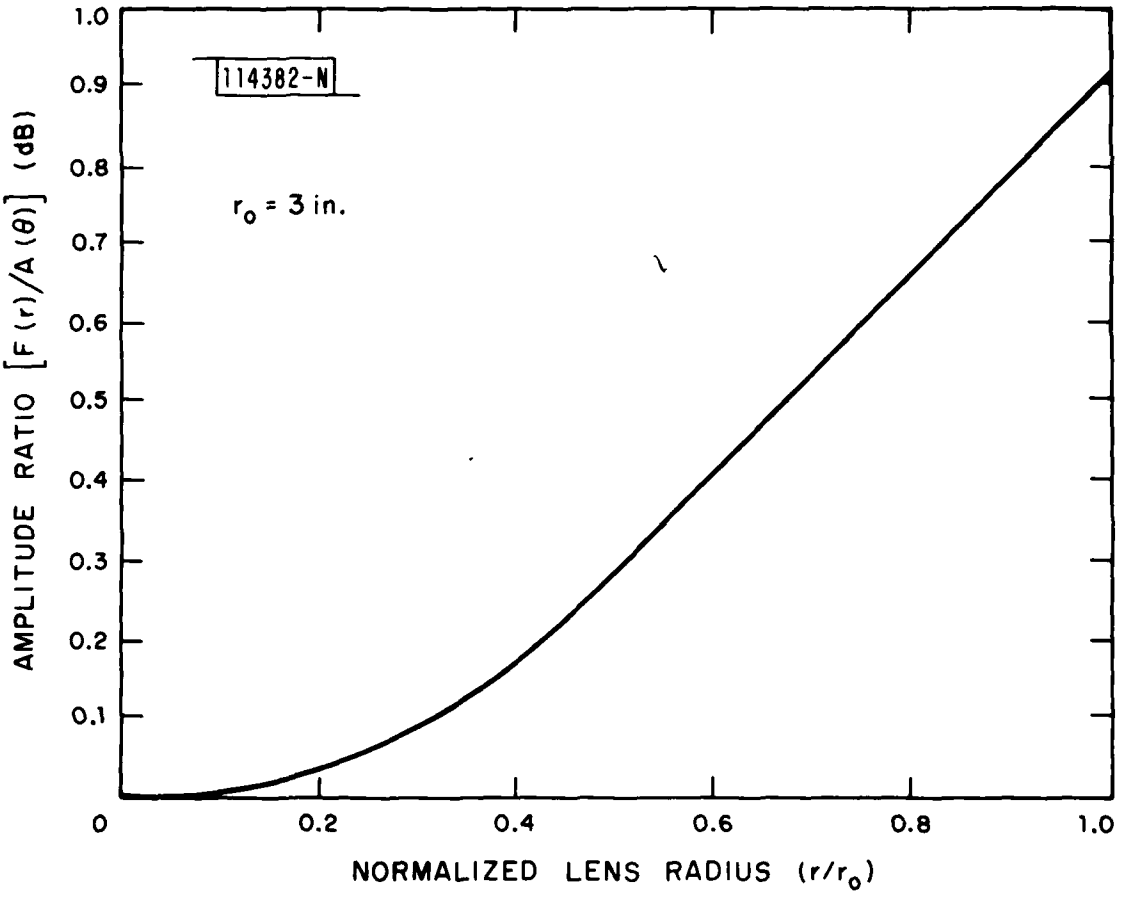

Fig. 9. Lens amplitude ratio F(r)/A(θ) vs normalized radius.

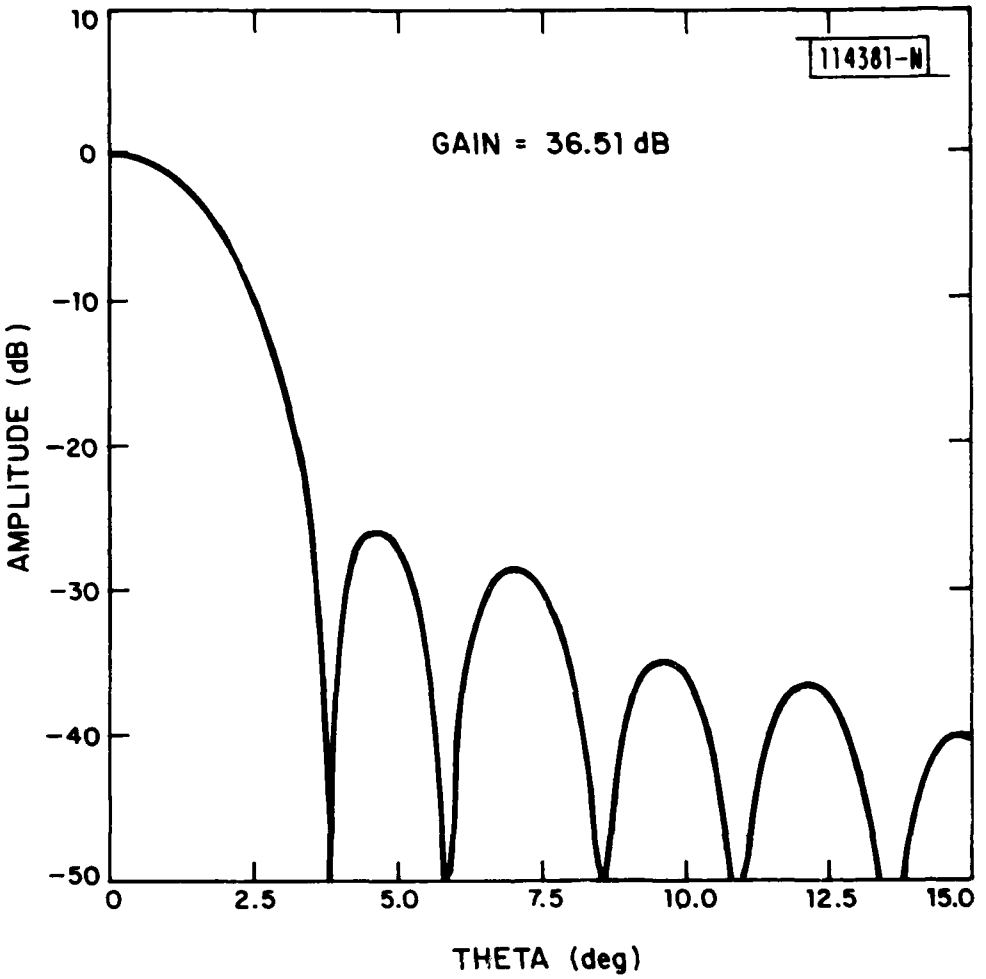

Fig. 10. Theoretical uplink radiation pattern (44.5 GHz) for lens antenna.

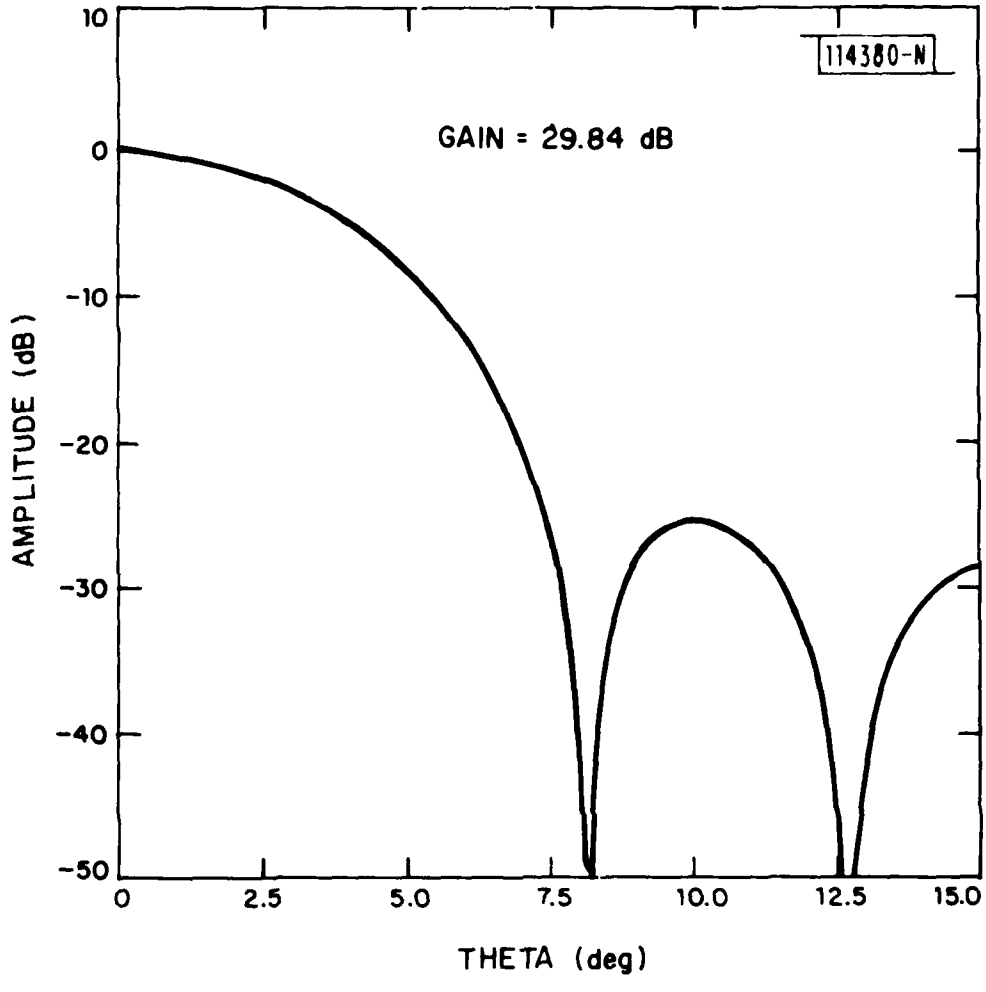

Fig. 11. Theoretical downlink radiation pattern (20.7 GHz) for lens antenna.

IV. MEASURED LENS RADIATION PATTERNS

A number of radiation patterns of the lens/horn antenna system were measured at the center and band edge frequencies of both the uplink and downlink bands (20.2, 20.7 and 21.2 GHz for the downlink; 43.5, 44.5 and 45.5 GHz for the uplink). These measurements were made with a linearly polarized transmitting antenna for electric-field polarizations which are either parallel or perpendicular to the x-z or y-z planes of scan (Fig. 2). Pertinent characteristics of these patterns, including 3 dB and 10 dB beamwidths, position and magnitude of the first sidelobe and null, and the angle θ_f beyond which all sidelobes are at least 30 dB down, are given in Table I for the downlink and Table II for the uplink at all three freqencies in each band. Graphs of selected radiation patterns, taken in the two principal planes with both E parallel and E perpendicular polarization, are presented for the uplink (Fig. 12; 44.5 GHz) and downlink (Fig. 13; 20.7 GHz) center frequencies in each band for the downlink. These tabular and graphical results show that the radiation patterns are essentially independent of frequency within each band and have a high degree of axial symmetry, regardless of polarization (E parallel and E perpendicular) or plane of scan (x-z and y-z). They also agree reasonably well on the downlink with the theoretical pattern (Fig. 11) relative to beamwidth and sidelobe structures. The measured 3 dB beamwidths vary between 5.6° and 6.4° over the band (20.2-21.2 GHz) while the first sidelobe level is less than -20 dB. Furthermore, the far-out sidelobes are all less than -34 dB for angles greater than 30°. These measurements compare favorably with the theoretical 3 dB beamwidth of 6.2° (Fig. 11) and first sidelobe level of -25 dB at 20.7 GHz.

The patterns for the uplink frequencies, on the other hand, exhibit some dissimilarity for different polarization and principal plane cuts. For both E perpendicular and E parallel polarizations, the 3 dB beamwidths vary between 2.8° and 3.5° over the band (43.5-45.5 GHz). This compares favorably with the theoretical 3 dB beamwidth of 3.0° at the center frequency (44.5 GHz). However, at this frequency the first sidelobe degenerates for E parallel

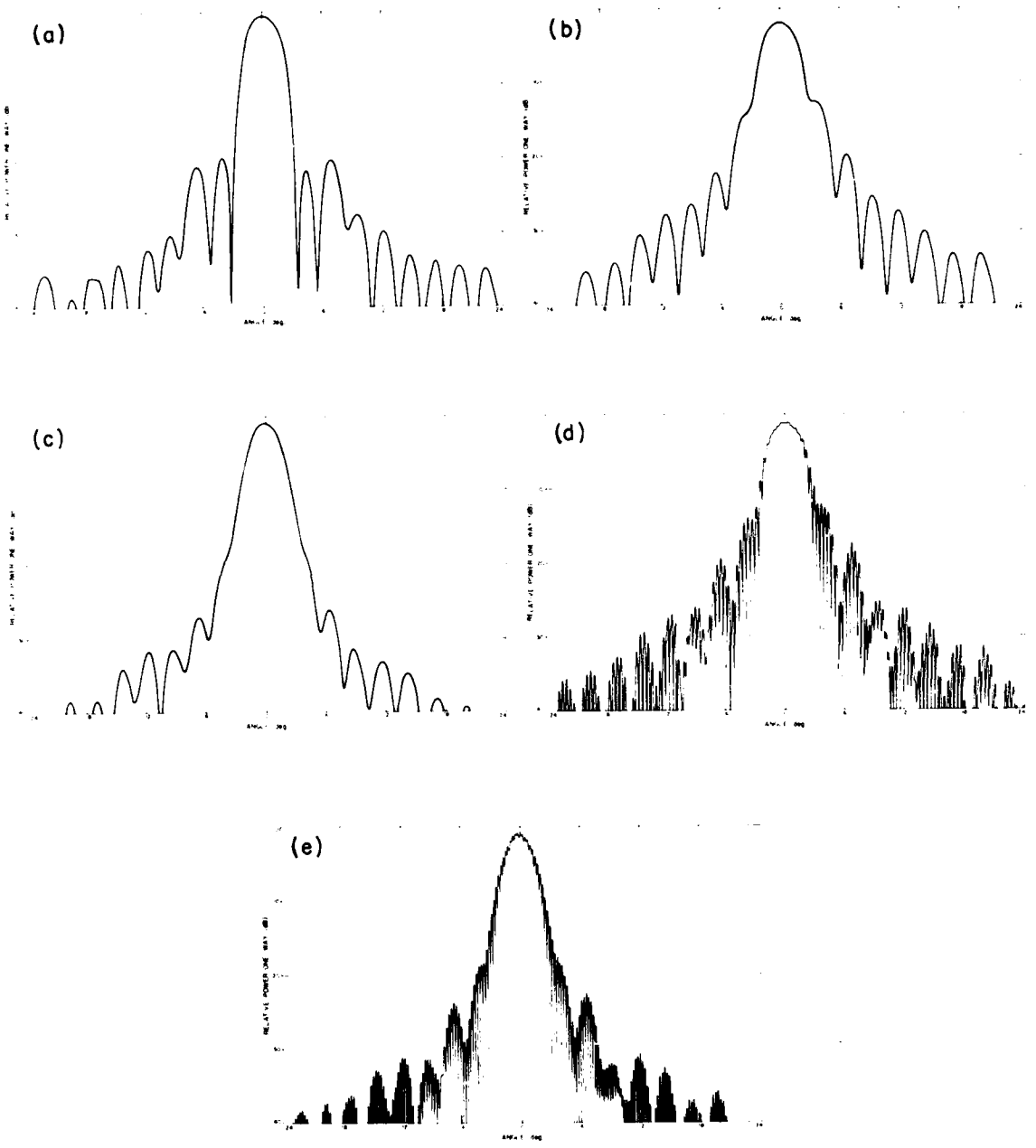

Fig. 12. Uplink lens radiation patterns (44.5 GHz): (a) X-Z plane, E perpendicular, (b) X-Z plane, E parallel, (c) Y-Z plane, E perpendicular, (d) X-Z plane, E rotating, (e) Y-Z plane, E rotating.

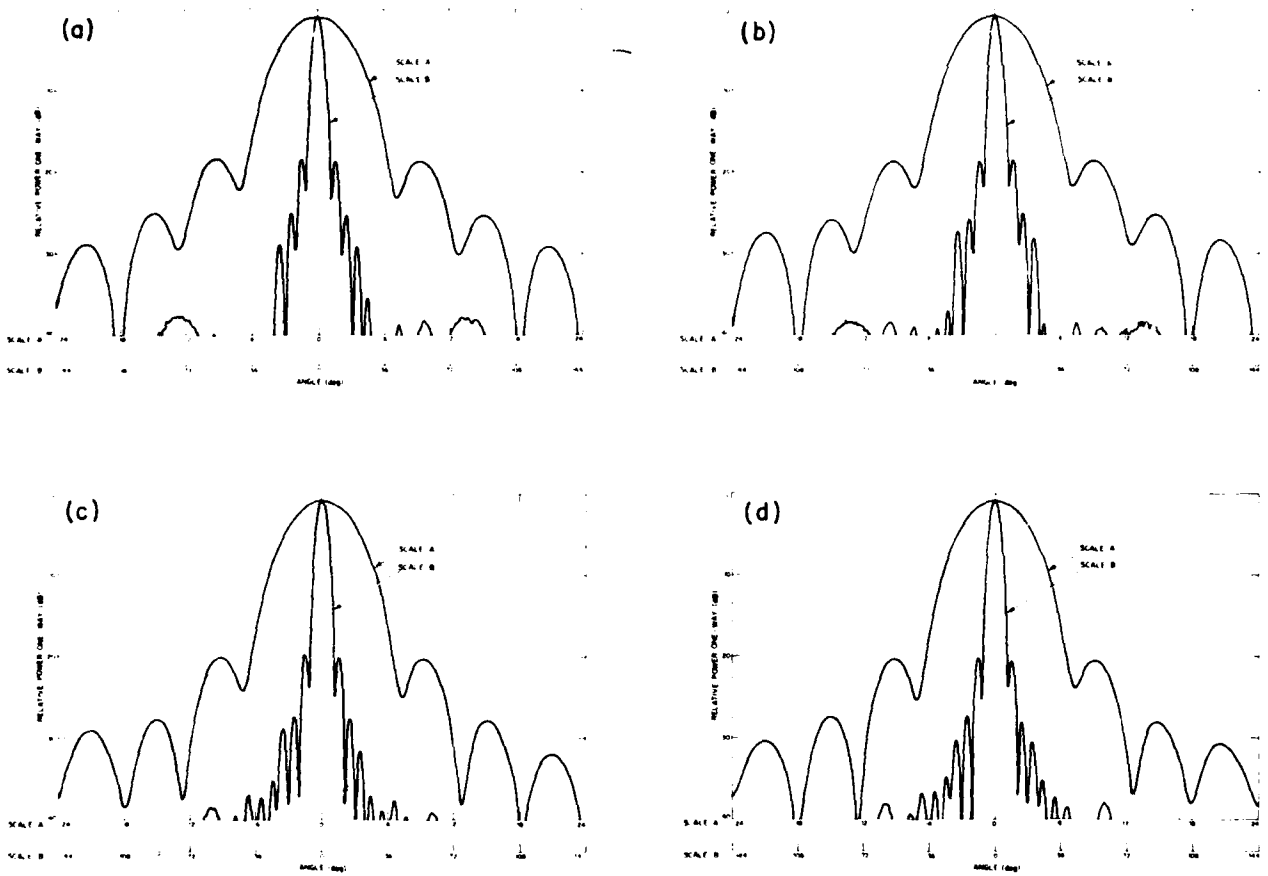

Fig. 13. Downlink lens radiation patterns (20.7 GHz): (a) Y-Z plane, E perpendicular, (b) X-Z plane, E perpendicular, (c) Y-Z plane, E parallel, (d) X-Z plane, E parallel.

TABLE I

DOWNLINK LENS RADIATION PATTERN CHARACTERISTICS

Freq. GHz	Pattern Plane	Pattern Polar.**	Beamwidth 3 dB (deg)	Beamwidth 10 dB (deg)	First Null Pos. (deg)	First Null Ampl. (dB)	First Sidelobe Pos. (deg)	First Sidelobe Ampl. (dB)	Far Sidelobes θ_f* (deg)
20.2	x-z	V	6.4	10.8	8.0	31	10.0	22	18
	y-z	V	6.4	10.8	8.0	28	10.0	23	18
	y-z	H	5.9	9.9	7.0	31	9.0	18	30
	x-z	H	5.7	9.9	6.9	32	9.0	18	28
20.7	y-z	V	6.1	10.4	7.2	21	9.3	18	28
	x-z	V	6.1	10.4	7.2	21	9.2	18	24
	x-z	H	5.9	10.1	7.2	23	9.1	19	28
	y-z	H	5.9	10.2	7.2	22	9.2	19	28
21.2	y-z	V	6.0	10.2	7.3	26	9.4	21	24
	x-z	V	5.9	10.1	7.2	26	9.3	20	24
	y-z	H	5.7	9.6	6.6	22	8.6	17	28
	x-z	H	5.6	9.4	6.5	22	8.6	17	24

*All sidelobes less than -30 dB for $\theta > \theta_f$

**Polarization of Incident E Field:

V - perpendicular to plane of scan

H - parallel to plane of scan

TABLE II

UPLINK LENS RADIATION PATTERN CHARACTERISTICS

Freq. GHz	Pattern Plane	Pattern Polar.**	Beamwidth 3 dB (deg)	Beamwidth 10 dB (deg)	First Null Pos. (deg)	First Null Ampl. (dB)	First Sidelobe Pos. (deg)	First Sidelobe Ampl. (dB)	Far Sidelobes θ_f* (deg)
43.5	x-z	V	2.8	4.8	3.3	∞	4.3	20	12
	x-z	H	3.0	5.3	4.0+	24	-	-	16
	y-z	V	2.8	4.7	3.4	35	4.3	20	12
	y-z	H	2.9	5.0	3.5+	17	-	-	18
44.5	x-z	V	3.5	5.1	3.4	35	4.2	19	15
	x-z	H	3.0	5.3	3.4+	12	-	-	14
	y-z	V	2.7	4.6	3.5	30	4.1	23	12
	y-z	H	3.1	5.3	3.7+	18	-	-	15
45.5	x-z	V	3.0	4.8	3.4	∞	4.2	22	22
	x-z	H	2.9	5.2	3.5+	15	-	-	12
	y-z	V	2.9	4.7	3.3	35	4.2	20	22
	y-z	H	2.9	4.8	3.0	15	3.8	14	20

+Shoulder on main beam

*All sidelobes less than -30 dB for $\theta > \theta_f$

**Polarization of incident E-field:

V - perpendicular to plane of scan

H - parallel to plane of scan

polarization (Fig. 12b) into a small shoulder at a level higher than -20 dB while for E perpendicular polarization (Fig. 12a) the null remains distinct at a level below -30 dB; these values compare to a theoretical first sidelobe level of -26 dB. The results indicate that the feedhorn possesses some degree of polarization-dependent astigmatism (defocussing) at the uplink frequencies. (This effect may be caused by the tapered dielectric rod wave launcher (Fig. 2) which, as an end-fire radiator, does not necessarily have a unique phase center for orthogonal polarizations.) However, the pattern distortion does not affect the overall performance or gain (Section V) of the antenna to any significant degree; for example, the far-out sidelobes on the uplink are excellent, being much less than -34 dB at all angles beyond 20°. As an additional check on these results, radiation patterns of the lens antenna were measured in the two principal planes, while the transmitting antenna was rapidly spinning, to determine its polarization characteristics. Typical patterns are shown in Figs. 12D and 12E at 44.5 GHz. The results, shown in Table III, are in consonance with the axial ratio measurements made on the feedhorn alone (Figs. 3 and 4) which remain below one dB for all frequencies. The corresponding polarization losses would be negligible (<0.1 dB) for all frequencies in both the uplink and downlink bands (Table III), when used with the circularly-polarized satellite antenna.

TABLE III

POLARIZATION LOSS OF LENS ANTENNA (θ=0°)

	Frequency (GHz)	Axial Ratio (dB)	Polarization Loss (dB)
	20.2	0.2	0.00
DOWNLINK	20.7	0.8	0.01
	21.2	0.5	0.00
	43.5	0.4	0.00
UPLINK	44.5	0.8	0.01
	45.5	1.0	0.01

V. ANTENNA GAIN CHARACTERISTICS

The on-axis gain of the lens antenna for circular polarization was determined for the uplink and downlink bands by adding 3 dB to the average value measured for two orthogonal linear polarizations. These results, together with corresponding calculations of directive gain and loss mechanisms, are shown in Table IV for the center and edge frequencies in each band. The differences between the measured gain and theoretical directivity can be attributed to several loss mechanisms (such as spillover, polarization mismatch and dissipative and reflective losses in the lens and feedhorn) and to possible measurement errors. The theoretical directive gain (D_T) is calculated from the lens aperture distribution F(r) which, in turn, is obtained from the measured horn pattern and Eqn. 5, and from the equation[9]

$$D_T = 8\pi^2 \left(\frac{r_o}{\lambda}\right)^2 \frac{|g(0)|^2}{\int_0^1 F^2(\tilde{r})\, \tilde{r}\, d\tilde{r}} \qquad (7)$$

where g(0) is the on-axis gain of the antenna and r_o the radius of the lens aperture.

For the uplink (44.5 GHz) the difference of 1.0 dB between the theoretical directivity of 36.5 dB and measured gain of 35.5 dB can be ascribed, in part, to an estimated spill-over loss of 0.3 dB, corresponding to 93% of the radiation from the feed being incident upon the lens. Other factors include an impedance mismatch and polarization losses of less than 0.2 dB and 0.1 dB, respectively. The difference of approximately 0.5 dB can be attributed to the dissipative and reflective losses in the lens and dissipation in the feedhorn. Overall antenna efficiency at 44.5 GHz is 71% (relative to a uniformly-illuminated 6"D aperture).

For the downlink (20.7 GHz), the difference of 0.3 dB between the theoretical directivity of 29.8 dB and measured gain of 29.5 dB is less than the sum of the spill-over loss (0.3 dB), mismatch loss (0.02 dB), and polarization loss (0.1 dB). Since some additional dissipative and reflective

TABLE IV

GAIN AND DIRECTIVITY OF LENS ANTENNA WITH FEED

	Uplink Frequency (GHz)			Downlink Frequency (GHz)		
	43.5	44.5	45.5	20.2	20.7	21.2
Directivity of 6" Lens (uniform aperture illumination)	36.8	37.0	37.2	30.2	30.4	30.6
Directivity of Lens (horn feed)	36.3**	36.5*	36.7**	29.6**	29.8*	30.0**
Gain of Lens (horn feed)+	35.3	35.5	35.8	28.8	29.5	29.2
Total Losses of Lens and Feed	1.0	1.0	0.9	0.8	0.3	0.8
Lens Antenna Efficiency	71%	71%	72%	72%	81%	72%
Spillover Losses	0.3	0.3	0.3	0.3	0.3	0.3
Mismatch Loss of Feed	0.08	0.05	0.20	0.10	0.03	0.20

Note: All values in dB

*Calculated from Eqn. (7) of text **Estimated from center frequency value
+Measured with two orthogonal linear polarizations and referred to circular polarization

losses must be present in the feed and lens, this anomalous result is attributed to either errors in measurement of the gain of the lens or of the radiation pattern of the feed (which is used to determine spillover loss). In any event, the overall antenna efficiency is on the order of 80% at 20.7 GHz and 72% at the band edges (20.2 and 21.2 GHz). These comparisons indicate that the losses in the lens do not exceed several tenths of a decibel in either the uplink or downlink frequency bands.

VI. CONCLUSIONS

The dielectric lens antenna with dual frequency feed has several advantages over hybrid or phased array systems for airborne satellite communication terminals. Its gain, which is close to the theoretical limits for its aperture size, remains constant as the antenna scans the upper hemisphere. Although it is not flush-mounted, its aerodynamic drag in a streamlined radome may not be significantly greater than the electronically-steerable arrays, which must be larger for equivalent electrical performance and require a cover of some type since they are generally non-conformal. Its low far-out sidelobes and high directivity in both bands result in low probability of intercept and resistance to jamming. As a mechanically steerable system, satellite acquisition can be achieved directly through the navigational aids on the aircraft and through step-scanning for final lock-on.

An improvement in this antenna design could be achieved if its overall length were reduced by bending the feed. The present design requires a minimum protrusion of the radome of 7" above the fuselage (recessing the lens by 1.5" into the aircraft with a corresponding gain degradation at zenith on the order of one decibel) and minimum cross-section dimension of 11". The corresponding dimensions with a folded feed would be 6" in height and 8" in cross section.

A second potential application for this type of antenna is in a low-data-rate terminal for ground vehicles. The antenna can be placed in a small armored rotatable turret on top of the vehicle (to provide protection against small arms fire) and scanned in azimuth and elevation for tracking the communication satellite. Although initial acquisition and synchronization with the satellite may be more difficult in a moving ground vehicle than in an aircraft, which has precise navigational aids, this problem is not expected to be particularly severe in view of the wide beamwidth (6°) on the downlink of the lens antenna.

ACKNOWLEDGMENTS

The authors acknowledge the support of John Russo who conducted the antenna measurements, John McCrillis who conducted the detailed measurements for the feed development, and Dennis Weikle who provided the engineering development of the lens antenna model.

REFERENCES

1. D. J. Frediani, "Technology Assessment for Future MILSATCOM Systems: The EHF Bands," Project Report DCA-5, Lincoln Laboratory, M.I.T. (12 April 1979), DDC AD-071886/6.

2. F. W. Cipolla, "A 7.5 GHz Microstrip Phased Array for Aircraft-to-Satellite Communication," Microwave J. 24, 75 (1981).

3. R. J. Mailloux, "Phased Array Aircraft Antennas for Satellite Communications," Microwave J. 20, 38 (1977).

4. J. T. Mayhan, and A. J. Simmons, "A Low-Sidelobe Antenna Radome Study at K_a-Band," Technical Note 1974-35, Lincoln Laboratory, M.I.T. (27 June 1974), DDC AD-785138/9.

5. S. Silver, Chapter 11 in Microwave Antenna Theory and Design, Vol. 12, (McGraw-Hill, New York, 1949).

6. Satellite Communications, H. L. VanTrees, Ed. (IEEE Press, New York, 1979), p. 588.

7. R. Price, "High Performance Corrugated Feed Horn for the Unattended Earth Terminal," COMSAT Tech. Rev. 4, 283 (1974).

8. S. Cornblett, Microwave Optics (Academic Press, New York, 1976), p. 200.

9. W. L. Stutzman and G. A. Thiele, Antenna Theory and Design, (Wiley and Sons, New York, 1981), p. 393.

UNCLASSIFIED

SECURITY CLASSIFICATION OF THIS PAGE *(When Data Entered)*

REPORT DOCUMENTATION PAGE		READ INSTRUCTIONS BEFORE COMPLETING FORM
1. REPORT NUMBER ESD-TR-82-002	2. GOVT ACCESSION NO.	3. RECIPIENT'S CATALOG NUMBER
4. TITLE *(and Subtitle)* Dielectric Lens Antenna for EHF Airborne Satellite Communication Terminals		5. TYPE OF REPORT & PERIOD COVERED Technical Report 6. PERFORMING ORG. REPORT NUMBER Technical Report 592
7. AUTHOR*(s)* Walter Rotman and Joseph C. Lee		8. CONTRACT OR GRANT NUMBER*(s)* F19628-80-C-0002
9. PERFORMING ORGANIZATION NAME AND ADDRESS Lincoln Laboratory, M.I.T. P.O. Box 73 Lexington, MA 02173-0073		10. PROGRAM ELEMENT, PROJECT, TASK AREA & WORK UNIT NUMBERS Program Element Nos. 63431F and 33601F Project Nos. 2029 and 6430
11. CONTROLLING OFFICE NAME AND ADDRESS Air Force Systems Command, USAF Andrews AFB Washington, DC 20331		12. REPORT DATE 16 February 1982 13. NUMBER OF PAGES 40
14. MONITORING AGENCY NAME & ADDRESS *(if different from Controlling Office)* Electronic Systems Division Hanscom AFB, MA 01731		15. SECURITY CLASS. *(of this report)* Unclassified 15a. DECLASSIFICATION DOWNGRADING SCHEDULE

16. DISTRIBUTION STATEMENT *(of this Report)*

Approved for public release; distribution unlimited.

17. DISTRIBUTION STATEMENT *(of the abstract entered in Block 20, if different from Report)*

18. SUPPLEMENTARY NOTES

None

19. KEY WORDS *(Continue on reverse side if necessary and identify by block number)*

EHF technology
satellite communications
lens antenna
millimeter wave antenna
aircraft antenna

20. ABSTRACT *(Continue on reverse side if necessary and identify by block number)*

A mechanically-steerable dielectric lens antenna, suitable for installation in an EHF airborne MILSATCOM terminal on high performance aircraft, was designed and tested. The antenna system consists of a six-inch diameter plano/convex lens with a dual frequency feed (43.5-45.5 GHz for the uplink and 20.2-21.2 GHz for the downlink). The measured gain and half-power beamwidths of the antenna system are 35.5 dB and a 3.2° for the uplink (44.5 GHz) and 29.5 dB and 6.0° for the downlink (20.7 GHz), corresponding to overall aperture efficiencies of 71% and 81%, respectively. The first sidelobes are −18 dB for the downlink and −20 dB for the uplink while the corresponding far-out sidelobes are less than −26 dB and −34 dB, respectively, for all angles beyond 18°. These characteristics are compatible with a high ECCM capability for an antenna of this size in an aircraft.

DD FORM 1 JAN 73 1473 EDITION OF 1 NOV 65 IS OBSOLETE

UNCLASSIFIED

SECURITY CLASSIFICATION OF THIS PAGE *(When Data Entered)*